

ANALYSIS OF IN-SITU ELECTRICAL CONDUCTIVITY DATA FROM THE HFIR TRIST-ER1 EXPERIMENT — S. J. Zinkle, W. S. Eatherly, L. L. Snead (Oak Ridge National Laboratory), T. Shikama (Tohoku University), and K. Shiiyama (Kyushu University)

OBJECTIVE

The objective of this work is to determine the existence or absence of bulk radiation induced electrical degradation (RIED) in neutron-irradiated Al_2O_3 .

SUMMARY

The current vs. applied voltage data generated from the HFIR TRIST-ER1 experiment have been analyzed to determine the electrical conductivity of the 15 aluminum oxide specimens and the MgO-insulated electrical cables as a function of irradiation dose. With the exception of the 0.05%Cr-doped sapphire (ruby) specimen, the electrical conductivity of the alumina specimens remained at the expected radiation induced conductivity (RIC) level of $<10^{-6}$ S/m during full-power reactor irradiation (10-16 kGy/s) at 450-500°C up to a maximum dose of ~3 dpa. The ruby specimen showed a rapid initial increase in conductivity to $\sim 2 \times 10^{-4}$ S/m after ~0.1 dpa, followed by a gradual decrease to $<1 \times 10^{-6}$ S/m after 2 dpa. Nonohmic electrical behavior was observed in all of the specimens, and was attributed to preferential attraction of ionized electrons in the capsule gas to the unshielded low-side bare electrical leads emanating from the subcapsules. The electrical conductivity was determined from the slope of the specimen current vs. voltage curve at negative voltages, where the gas ionization effect was minimized. Dielectric breakdown tests performed on unirradiated mineral-insulated coaxial cables identical to those used in the HFIR TRIST-ER1 experiment indicate that the electrical shorting which occurred in many of the high voltage coaxial cables during the 3-month irradiation is attributable to thermal dielectric breakdown in the glass seals at the end of the cables, as opposed to a radiation-induced electrical degradation (RIED) effect.

PROGRESS AND STATUS

Introduction

As reported in a preceding semiannual progress report [1] a collaborative DOE/Monbushto irradiation experiment has been completed which measured the in-situ electrical resistivity of 12 different grades of aluminum oxide during HFIR neutron irradiation at 450-500°C. The main objective of the Temperature Regulated In-Situ Test - Electrical Resistivity (TRIST-ER1) experiment was to determine if radiation induced electrical degradation (RIED) occurred in several different grades of aluminum oxide during irradiation in a fusion-relevant irradiation environment up to relatively high doses. According to previous studies performed primarily with 1.8 MeV electrons, RIED is expected to be most pronounced at temperatures between 300 and 600°C and at applied voltages >100 V/mm, with an apparent maximum degradation rate occurring near 450°C [2,3]. The HFIR TRIST-ER1 experiment was performed at an irradiation temperature of 450-500°C with a dc electric field of 200 V/mm.

The preliminary analysis of the electrical data reported previously [1] did not show any evidence for bulk RIED in the high-purity alumina specimens above the expected RIC level of $\sim 1 \times 10^{-6}$ S/m during full-power irradiation up to a maximum dose of 3 dpa. However, there were several issues which were not satisfactorily addressed in this preliminary analysis: (1) only a limited analysis of the electrical conductivity of the specimens at selected times was performed for the previous report, (2) the cause of the eventual failure of 10 of the 15 coaxial cables during the 3-1/2 month irradiation was uncertain (it was speculated in the preceding report to be due to dielectric breakdown in the glass seals at the cable termination), and (3) the physical mechanism(s) responsible for the observed nonohmic electrical behavior were uncertain. Recent progress toward resolution of these issues is summarized in this report.

Experimental Procedure

The experiments were performed in the Temperature-Regulated In-Situ Test (TRIST) facility located in a Removable Beryllium position of the High Flux Isotope Reactor (HFIR) at Oak Ridge National Laboratory (ORNL). A total of 15 specimens were irradiated in the in-situ electrical conductivity capsule. The specimen matrix included 12 different grades of polycrystal and single crystal alumina (Table 1) in order to confirm published studies which suggested that the threshold dose for initiation of RIED depends on specimen purity [3,4]. The TRIST-ER1 experiment was performed following the guidelines outlined in ASTM Standard Test Method for DC Resistance or Conductance of Insulating Materials (ASTM D257-91), and in accordance with the stringent experimental technique conditions adopted by the participants to an IEA ceramic insulator workshop held in Stresa, Italy in September 1993 [5]. In particular, the electrical contacts were brazed onto the specimen surface so that contact resistances were negligible, and the leakage resistances between the back (high voltage) and low voltage guard and center electrodes was measured periodically throughout the irradiation. The specimen temperatures were monitored continuously by two thermocouples located in each subcapsule. The sample temperatures were controlled by adjusting the composition of a flowing mixture of helium and neon in the control gas gap between the subcapsules and the holder sleeve [1,6]. The measured irradiation temperatures for the 15 subcapsules ranged from ~440 to 500°C, depending on the subcapsule position. Details of the irradiation temperature history are described elsewhere [6]. All of the subcapsules were sealed to minimize the amount of surface contamination buildup during irradiation.

The specimen matrix included 7 high-purity single crystal alumina specimens produced by two different manufacturers with different crystallographic orientations (Table 2). Seven polycrystalline alumina specimens with impurity contents ranging from 0.1 to 3% were included in the capsule, along with a 0.05% Cr-doped single crystal alumina (ruby) specimen. Two of the single crystal specimens and one of the polycrystal specimens (subcapsules 11, 12 and 15) were irradiated without dc bias and served as control specimens for the RIED experiment. The alumina specimens were irradiated as disks with dimensions of 8.5 mm diameter by 0.75 mm thick. A 1.1 mm OD triaxial MgO powder-insulated cable with a copper center wire and a braided copper sheath was used as the low-side data lead from each subcapsule. A 1.6 mm OD coaxial MgO powder-insulated cable with a copper center conductor was used as the power lead. The leads for the coax and triax cables were torch-brazed and spot welded to the appropriate Ni wires from each subcapsule. The mineral insulated (MI) cables were connected to polymer-insulated coax and triax cables near the top of the HFIR pressure vessel. The series line resistances of the coaxial and triaxial cables were all ~3-5 Ω . Further experimental details are given elsewhere [1].

Data acquisition and control was performed using a National Instruments Labview III program running on a Macintosh computer. A Keithley 7002 matrix switch system (containing Keithley 7169A switch cards on the high side and 7058 switch cards on the low side) was used to switch the specimen leads to the appropriate electrical instruments. A dc potential of 150 V was continuously supplied to the brazed base surface of 12 of the specimens (except for brief periods when electrical measurements were taken) by two HP 6035A power supplies, producing an electric field of 200 V/mm in the specimens. As described elsewhere [1], several different types of electrical measurements were performed on the specimens in order to differentiate between bulk conductivities and surface conductances. These tests included frequent measurement of the specimen and guard ring currents at 100 V and periodic measurement of the ohmic nature of the electrical currents in the alumina samples and coaxial MI cables over a typical potential range of +100 V to -100V. Diagnostic measurements were also performed periodically which allowed the surface resistance and cable insulation conductivities to be measured. For each electrical measurement, a settling time of 10 to 30 seconds was typically used from the time the specimen was switched to the power supply until an electrical current was measured in order to eliminate signal noise associated with the cable and specimen capacitance. During the reactor startup and shutdown, a settling time of 5 to 10 seconds was typically used in order to obtain data more rapidly.

The irradiation was accomplished over a time period of about three and one half months, and involved three irradiation cycles (cycles 344-346, each ~26 days long) of the HFIR reactor operating at 85 MW. The electrical conductivity of the specimens was measured before, during and following each of the three HFIR irradiation cycles. The specimen temperatures ranged from 30 to 50°C when the reactor was off, and between 50 and 170°C (depending on the control gas mixture) when the reactor was at 10% power. The irradiation temperature was maintained at 440 to 500°C for all 15 specimens during full-power irradiation. The full-power reactor ionizing dose rate [6] was 10 to 16 kGy/s and the average displacement damage rate was ~2.4 to 4.3×10^{-7} dpa/s, with the lowest dose rates obtained for subcapsules 1 and 15 and the highest dose rate for subcapsule 8 (Table 2). The ionizing dose rate in the core with the reactor turned off (spent fuel removed) was ~10 Gy/s.

During the first five days of the irradiation, all of the biased specimens which were not undergoing an electrical measurement were left connected to the 150 V dc bias from the HP power supplies. This was performed in order to minimize the amount of time that the "biased" samples were exposed to irradiation with the electric field turned off. However, this arrangement had a disadvantage of producing large (~0.1-1 A) transient electrical current spikes in the coax cables during the switching operations, particularly when specimens were switched from an ohmic check measurement at -100 V back into the bias circuit at +150 V. Several of the coaxial cables failed (electrical short) during the first few days of irradiation, presumably due to these high transient currents. The Labview program was modified after five days of irradiation to shut off the 150 V bias during electrical measurements, and to slowly ramp the power supply from 0 to 150 V when the bias was reapplied following completion of a set of electrical measurements. The frequency of electrical measurements was reduced to ~ two per day when this change was implemented in order to minimize the amount of time that specimens were irradiated without the 150 V bias. The 150 V potential was applied to the biased specimens ~98% of the total irradiation time. Several additional coaxial cables shorted during the subsequent 3 months of irradiation, although the frequency of failure was much lower compared to the first 5 days of irradiation.

In order to evaluate whether the coaxial cable shorting was associated with normal dielectric breakdown effects versus a radiation-induced phenomenon, the dielectric breakdown strength was measured on 6 spare unirradiated coaxial cables that were produced by the vendor in the same batch as the HFIR cables. These electrical breakdown measurements were performed at either room temperature or at 200°C in an open-air furnace with a Keithley 237 Source-Measure Unit as the power supply. The temperature of 200°C corresponds to the maximum expected operating temperature of the coaxial cables in the TRIST-ER1 capsule during full-power irradiation.

Results

Nonohmic electrical behavior

Figure 1 shows the result of an ohmic check performed on a UV-grade sapphire specimen (sample #1) during full-power HFIR irradiation. The electrical current for positive applied potentials was significantly higher than the magnitude of the electrical current for negative applied potentials. Variation of the settling time between voltage application and current measurement (τ_{RC}) from 5 s to 180 s had no effect on the shape of the current vs. voltage curve. The calculated RC time constant for the HFIR electrical circuit was mainly determined by the capacitance of the coaxial cable (7 nF) which was three orders of magnitude larger than the capacitance of the alumina specimens (~7 pF). Using the typical measured resistances of the coaxial cables and alumina specimens during full-power irradiation, the calculated RC time constant for the HFIR circuit was ~10 ms, which is orders of magnitude smaller than the settling times used for the HFIR measurements. The ohmic check measurements were generally obtained by first applying a positive voltage, followed by progressively decreasing voltages. However, a similar current vs. voltage curve was also obtained when the voltage application sequence was reversed (i.e., initially applying negative voltages, followed by progressively more positive voltages). The asymptotic slope of the ohmic check curve at the highest positive voltages was typically between two and ten times larger than the slope measured at negative voltages.

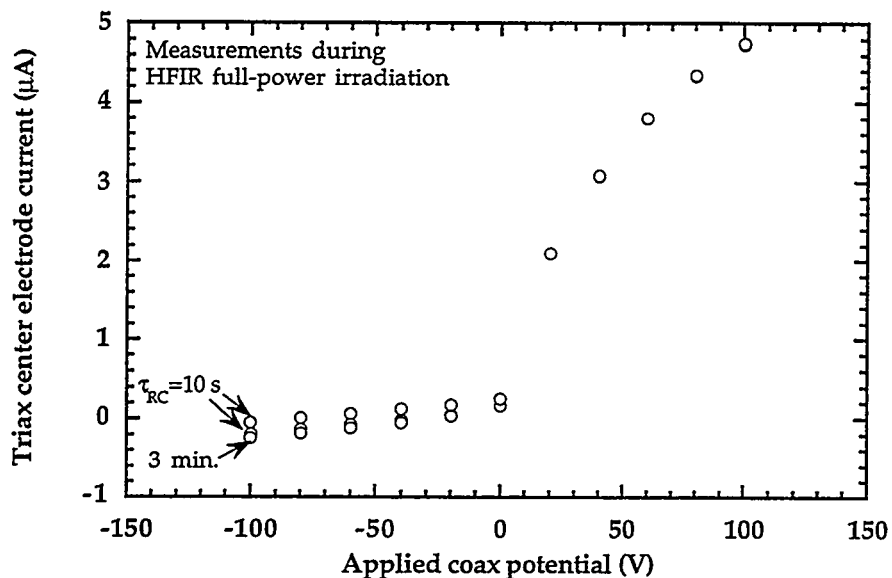


Fig. 1. Effect of RC wait time (τ_{RC}) on the electrical response of Crystal Systems sapphire (UV grade, a-axis orientation) during full-power HFIR irradiation at $\sim 450^\circ\text{C}$. The $\tau_{RC}=10$ s measurements were performed immediately before and after the $\tau_{RC}=3$ min measurements.

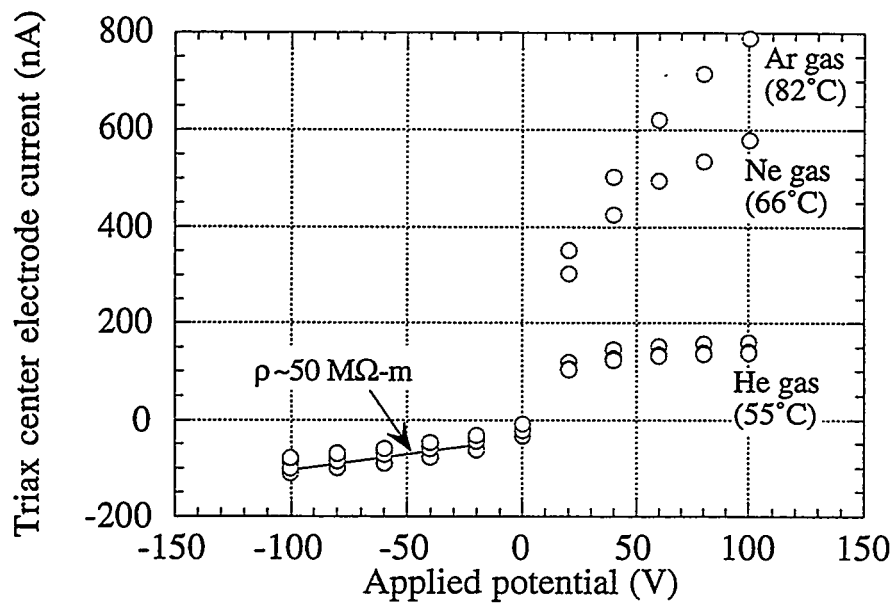


Fig. 2. Electrical response of Crystal Systems UV grade sapphire (c-axis orientation, sample #2) approximately 1 h after completion of the first HFIR irradiation cycle.

Table 1. Ion pair production rates for several gases [7]

Gas	K (ion pairs/cm ³ -Gy)
He	2.3×10^{10}
Ne	7.0×10^{10}
Ar	17.7×10^{10}
air	21.5×10^{10}

As noted in our previous semiannual report [1], a pronounced increase in the measured current for positive applied voltages (but not for negative voltages) was observed in all samples on several occasions prior to the initial startup of the HFIR reactor. From a comparison with the operating history of the TRIST-ER1 capsule gas handling system, it was determined that this increase in current for positive voltages coincided with switching from the default He gas mixture to an Ar/He gas mixture. Figure 2 shows the results of several ohmic check measurements that were performed on a UV-grade sapphire specimen following the end of the first HFIR cycle (~1 dpa). The capsule gas mixture (used to control the specimen temperatures during full-power irradiation) was changed in the sequence He->Ne->Ar in an attempt to increase the specimen temperature and thereby measure the temperature-dependent electrical conductivity of the irradiated specimens in a relatively low ionizing radiation field compared to full-power reactor operation. Only a small elevation in temperature was achieved by this change in gas mixture, due to the low residual nuclear heating rate after reactor shutdown and the relatively small gas gaps (~20-100 μm) in the HFIR TRIST-ER1 design. The radiation induced conductivity obtained from the slope in the negative quadrant of the current vs. voltage curves was $\sim 2 \times 10^{-6}$ S/m for all three gas mixtures. On the other hand, the slope of the current vs. voltage curve in the positive quadrant was dependent on the gas environment, with the highest slope occurring for Ar and the lowest slope occurring for He.

The conductivity of an ionized gas is given by $\sigma = n_e e \mu_e + n_i e \mu_i$, where n_e and n_i are the density of ionized electrons and ions (assumed singularly charged), respectively, e is the electron charge, and μ_e and μ_i are the electron and ion mobilities, respectively [8]. Since the ion mobility is much smaller than the electron mobility, $\mu_i \sim 10^{-3} \mu_e$ [7,8], the ion contribution to the current can be neglected. Therefore, the gaseous current should be mainly evident for positive applied voltages (due to preferential attraction of electrons) and should be orders of magnitude smaller for negative voltages. The electrical conductivity in most gases has been found to be proportional to ionizing dose rate up to $\sim 10^{10}$ Gy/s, due to the high electron reattachment rate (typical free electron lifetimes are ~ 10 ns) [9]. The electrical conductivity of the ionized gas can be described by the following equation [10].

$$\sigma_e = n_e e \mu_e = K D e \mu_e / \alpha \quad (1)$$

where K is the production rate for ion pairs, D is the ionizing dose rate and α is the electron attachment rate. The electrical conductivity of air for dose rates relevant to full-power HFIR irradiation (16 kGy/s) is $\sigma_e = 3.7 \times 10^{-6}$ S/m, which is comparable to the RIC in Al_2O_3 . Table 1 summarizes the ion pair production rate for different gases [7]. It can be seen that Ar would produce the highest gas conductivity and He would produce the lowest gas conductivity among the 3 noble gases, which is similar to the experimental results for positive voltages shown in Fig. 2. Therefore, the observations that the nonohmic behavior occurs mainly for positive applied voltages and that the relative magnitude of the current agrees with the expected RIC values for different gas species both suggest that the observed non-ohmic electrical behavior during HFIR irradiation is due to preferential attraction of ionized electrons in the capsule gas to the unshielded portion of the "low-side" electrical leads.

Whereas gas conductivity effects appear to qualitatively explain much of the observed nonohmic behavior in the TRIST-ER1 experiment, quantitative agreement is more difficult to obtain. It should be noted that the specimen electrical currents were measured on the low side (i.e., near electrical ground). The voltage change in the low-side triaxial cable was on the order of 0.1 mV as the coaxial voltage was changed between 100 V and -100 V. Furthermore, only ~1 to 2 cm of the

triaxial electrical lead from each subcapsule was unshielded. Considering the ~6 orders of magnitude smaller electric field for the gas compared to the alumina specimen and the comparable areas of the bare triaxial center lead and the alumina specimen electrodes, the calculated current in the triaxial cable center lead would be expected to be dominated by the alumina specimen rather than gas conductivity effects.

The shape of the current vs. voltage plots shown in Figs. 1 and 2 are qualitatively very similar to Langmuir probe current-voltage plots obtained in plasma physics studies of ionized gases [11]. Since a gas ionized by radiation is essentially a weakly ionized plasma, this plasma physics approach may be useful for the analysis of the nonohmic TRIST-ER1 electrical data. The nonohmic behavior in the Langmuir probe plots has been shown to be due to the difference in the electron and ion fluxes incident on the wire probe, the ratio of which is proportional to $(m_i/m_e)^{1/2}$ where m_i and m_e are the ion and electron masses. Further analysis is necessary to determine whether the plasma physics equations developed for Langmuir probes can quantitatively describe the HFIR TRIST-ER1 electrical data.

In the following sections, the electrical conductivity was calculated from the slope of the current vs. voltage plots for applied coaxial cable voltages less than -20 V. The surface leakage resistances between the center, guard and back electrodes were routinely measured and compared with the apparent bulk resistance to determine if surface leakage currents were affecting the conductivity measurements, using the equations given by Kesternich et al. [12].

Time-dependent electrical conductivity

Figure 3 shows the electrical conductivity measured on UV grade Crystal Systems sapphire before and during the first few days of the first HFIR cycle. The measured electrical conductivity outside of the reactor core was $<10^{-10}$ S/m, which is at the resolution limit of the electrical equipment used for the HFIR TRIST-ER1 experiment (due to the ~1 T Ω leakage resistance of the scanner cards in the matrix switch system). The electrical conductivity increased to $\sim 4 \times 10^{-9}$ S/m when the capsule was inserted into the HFIR core prior to the start of the radiation (residual background radiation dose rate of ~10 Gy/s). The electrical conductivity was $\sim 4 \times 10^{-8}$ S/m and $\sim 1.2 \times 10^{-7}$ S/m for 10% power and full power irradiation conditions. Figure 4 shows the electrical conductivity of a regular grade of Crystal Systems sapphire measured before, during and after the three HFIR reactor cycles. It can be seen that the electrical conductivity of the specimen never exceeded $\sim 3 \times 10^{-7}$ S/m during full-power irradiation at an ionizing dose rate of ~12 kGy/s during the 3 HFIR irradiation cycles. Following the irradiation, the electrical conductivity of the specimen returned to a value that was similar to the preirradiation value (limited by the leakage resistance in the TRIST-ER1 electrical equipment).

Table 2 summarizes the electrical conductivity measurements for the 15 alumina specimens before and during the initial stages of the first HFIR irradiation cycle. The preirradiation in-core electrical conductivity ranged from $\sim 3 \times 10^{-10}$ S/m to 4×10^{-9} S/m for the different specimens. The electrical conductivity at 10% reactor power (1.0-1.6 kGy/s) ranged from 4×10^{-8} S/m to 2×10^{-7} S/m. The high-purity single crystal specimens generally had higher RIC values than the polycrystal specimens for both of these irradiation conditions. The RIC values for full-power irradiation ranged from 1.2×10^{-7} to 1×10^{-6} S/m, with no consistent difference between the single crystal and polycrystal specimens.

Table 3 shows the corresponding electrical conductivity values measured for the 15 MgO-insulated coaxial cables. The electrical conductivity was determined from the slope of the power supply current vs. voltage plots at voltages less than -20 V. The well-known geometry factor for coaxial cables, $R/\rho = \ln(b/a)/2\pi L$, was used to convert the measured resistance (R) to resistivity (ρ) values, where b and a are the outer and inner diameters of the MgO insulation and L is the length of the coaxial cable that was in the HFIR core region. The value of L used for the conductivity calculation ranged from 5 cm for cable #1 to 45 cm for cable #15. The RIC values for the coaxial

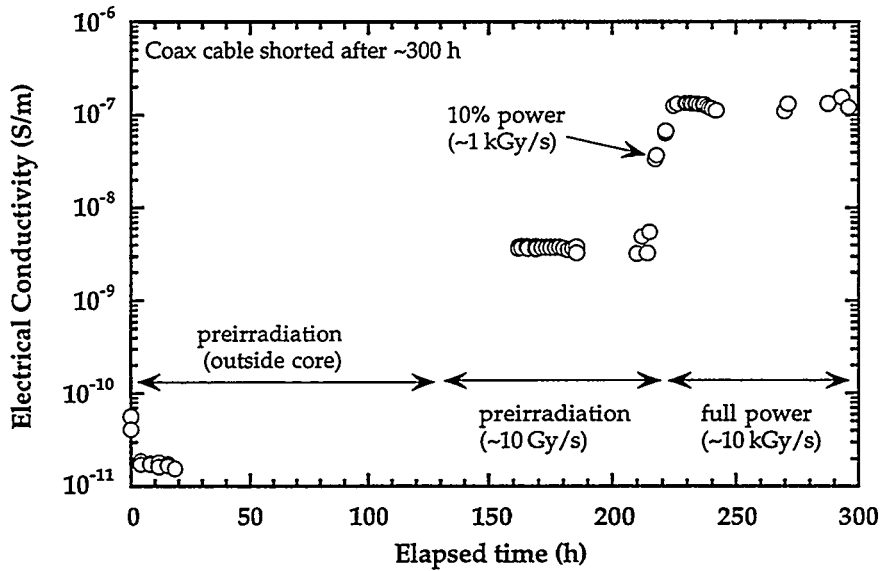


Fig. 3. Electrical conductivity of Crystal Systems sapphire (UV grade, a-axis orientation, specimen position #1) prior to and during the first HFIR irradiation cycle.

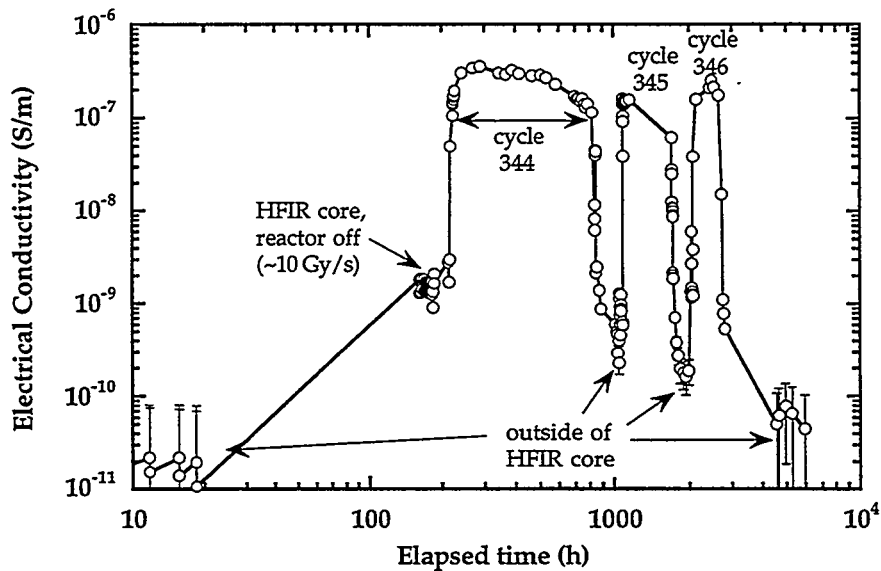


Fig. 4. Electrical conductivity of Crystal Systems sapphire (regular grade, c-axis orientation, specimen position #3) prior to, during and following the three HFIR irradiation cycles.

Table 2. Summary of HFIR TRIST-ER1 electrical conductivity measurements at startup

Position # and material	Electrical Conductivity (S/m)		
	In-core, reactor off (10 Gy/s, 60°C)	10% power (1-1.6 kGy/s, 170°C)	100% power (10-16 kGy/s, 450°C)
1. CSI sapphire, UV, a-axis	4×10^{-9}	4×10^{-8}	1.2×10^{-7}
2. CSI sapphire, UV, c-axis	3×10^{-9}	6×10^{-8}	3×10^{-7}
3. CSI sapphire, regular, c-axis	2×10^{-9}	5×10^{-8}	3×10^{-7}
4. CSI sapphire, regular, a-axis	1.5×10^{-9}	9×10^{-8}	4×10^{-7}
5. Vitox (99.9% purity)	$(<7 \times 10^{-8})^*$	$(\leq 4 \times 10^{-7})^*$	1×10^{-6}
6. Kyocera A480 (99.9% purity)	3×10^{-10}	1×10^{-7}	1×10^{-6}
7. Wesgo AL300 (97% purity)	5×10^{-10}	2×10^{-7}	5×10^{-7}
8. Kyocera A479 (99.0% purity)	3×10^{-10}	6×10^{-8}	3×10^{-7}
9. Coors AD998 (99.8% purity)	3×10^{-10}	1×10^{-7}	—
10. Wesgo AL995 (99.5% purity)	3×10^{-10}	6×10^{-8}	8×10^{-7}
11. Wesgo AL995 (99.5% purity)	4×10^{-10}	4.5×10^{-8}	2×10^{-7}
12. CSI sapphire, regular, c-axis	2×10^{-9}	6×10^{-8}	3×10^{-7}
13. Un. Carbide Cr-doped sapphire	1×10^{-9}	7×10^{-8}	2×10^{-7}
14. Kyocera SA100, [1102]	3×10^{-9}	7×10^{-8}	2×10^{-7}
15. Kyocera SA100, [1102]	$(<1 \times 10^{-7})^*$	$(<1 \times 10^{-6})^*$	$(<3 \times 10^{-6})^*$

*values in parenthesis denote upper limits to bulk conductivity due to high surface leakage currents

Table 3. Summary of measured in-core conductivities (S/m) for the coax cables at the start of the HFIR irradiation (from the negative quadrant of the ohmic check plots). The data marked with an asterisk denote values that are a upper limit to the bulk conductivity due to low (<1 MΩ) surface leakage resistances (measured with the reactor turned off)

HFIR position	Preirradiation (10 Gy/s, 50°C)	10% power, 0 dpa (1-1.6 kGy/s, 170°C)	Full power, 0 dpa (10-16 kGy/s, 440-500°C)	Full power, 1st cycle avg. (10-16 kGy/s, 440-500°C)
1.	$(<1.5 \times 10^{-6})^*$	$\sim 6 \times 10^{-6}$	$\sim 6 \times 10^{-6}$	$\sim 6 \times 10^{-6}$
2.	$(<2 \times 10^{-7})^*$	$\sim 1 \times 10^{-6}$	$\sim 4 \times 10^{-6}$	$\sim 2 \times 10^{-5}$
3.	$\sim 2 \times 10^{-9}$	$\sim 2 \times 10^{-7}$	$\sim 5 \times 10^{-7}$	$\sim 2 \times 10^{-6}$
4.	$(<5 \times 10^{-8})^*$	$\sim 4 \times 10^{-7}$	$\sim 3 \times 10^{-6}$	—
5.	$(<4 \times 10^{-5})^*$	$(<2 \times 10^{-5})^*$	$(<5 \times 10^{-5})^*$	$(<5 \times 10^{-5})^*$
6.	$(<1.5 \times 10^{-8})^*$	$\sim 2.5 \times 10^{-7}$	$\sim 2 \times 10^{-6}$	—
7.	$\sim 2 \times 10^{-10}$	$\sim 8 \times 10^{-8}$	$\sim 5 \times 10^{-7}$	$\sim 5 \times 10^{-7}$
8.	$(<1 \times 10^{-7})^*$	$\sim 4 \times 10^{-7}$	$\sim 8 \times 10^{-7}$	$\sim 4 \times 10^{-7}$
9.	$(<3 \times 10^{-7})^*$	$\sim 2 \times 10^{-7}$	$\sim 5 \times 10^{-7}$	$\sim 4 \times 10^{-7}$
10.	$(<1 \times 10^{-7})^*$	$\sim 1 \times 10^{-7}$	$\sim 1 \times 10^{-5}$	—
11.	$\sim 1.5 \times 10^{-9}$	$\sim 5 \times 10^{-8}$	$\sim 5 \times 10^{-7}$	$\sim 2 \times 10^{-7}$
12.	$\sim 1 \times 10^{-9}$	$\sim 7 \times 10^{-8}$	$\sim 1 \times 10^{-6}$	$\sim 2 \times 10^{-6}$
13.	$(<2 \times 10^{-8})^*$	$\sim 2 \times 10^{-7}$	$\sim 5 \times 10^{-7}$	$\sim 2 \times 10^{-6}$
14.	$\sim 5 \times 10^{-10}$	$\sim 5 \times 10^{-8}$	$\sim 3 \times 10^{-7}$	—
15.	$(<5 \times 10^{-5})^*$	$(<7 \times 10^{-5})^*$	$(<1 \times 10^{-4})^*$	$(<3 \times 10^{-5})^*$

cables were comparable or somewhat higher than that measured for the alumina specimens. The measured RIC values for the coaxial cables are an upper limit to the bulk conductivity, since possible effects associated with surface leakage currents were not measured for the cables. Figure 5 shows the time-dependent electrical conductivity of the coaxial cable for sample #3. The apparent electrical conductivities measured with the reactor off were much higher than the corresponding values for the Al_2O_3 specimens, most likely because of surface leakage currents at the cable termination. Anomalously high leakage currents were observed in coax cable #3 during most of the shutdown period between HFIR cycles 345 and 346, suggesting that some degradation (surface or bulk) may have occurred in the MgO insulation or glass seal. However, measurements made several months following the completion of the third irradiation cycle produced apparent conductivities similar to the preirradiation value.

Figure 6 shows the time dependent electrical conductivities for two polycrystalline alumina specimens whose coaxial cables shorted during the second HFIR irradiation cycle. In both specimens, the electrical conductivity was essentially constant during full-power irradiation with values near 2 to 6×10^{-7} S/m. There was no evidence of degradation of the bulk conductivity of either specimen prior to the shorting in the electrical cables. The cable for the Wesgo AL300 specimen shorted during an ohmic check measurement with an applied voltage of -100 V. The electrical measurements made at $+100$ to -80 V in this measurement sequence did not indicate any unusual behavior in either the coaxial cable or the alumina specimen.

Figures 7-12 show electrical conductivity vs. displacement damage dose plots for several of the alumina specimens irradiated in the HFIR TRIST-ER1 experiment. The dose level was obtained by using the following conversion from neutron fluence: $1 \text{ dpa} = 1 \times 10^{25} \text{ n/m}^2$ ($E > 0.1 \text{ MeV}$). Only measurements made during full-power reactor operation are plotted in these figures in order to maintain roughly constant dose rates. In several cases (e.g., Figs. 7,8), the electrical conductivity increased slightly by a factor of 2 to 5 during the first few days of HFIR irradiation (up to ~ 0.1 dpa), and this was followed by a gradual decrease in electrical conductivity at higher doses. None of the polycrystalline alumina or high-purity sapphire specimens irradiated with a dc electric field of 200 V/mm exhibited a full-power electrical conductivity above $\sim 10^{-6}$ S/m during this experiment, despite the fact that several specimens achieved damage levels of nearly 3 dpa. Pronounced RIED ($\sigma_e > 10^{-5}$ S/m) occurred for doses of less than 10^{-4} dpa in several previous electron irradiation studies performed on high-purity sapphire and Vitox polycrystalline alumina [3]. When corrections for the high dose rate in the HFIR irradiation compared to the electron irradiations are taken into account, pronounced RIED would have been predicted to occur at HFIR doses above ~ 0.01 dpa according to extrapolations from the electron irradiation data base [3]. Therefore, it appears that the as-yet uncertain physical mechanisms responsible for RIED during electron irradiation may not be present during neutron irradiation up to relatively high doses.

As shown in Fig. 12, a large increase in the electrical conductivity of the 0.05% Cr-doped sapphire (ruby) specimen occurred during the first three days of HFIR irradiation. The electrical conductivity reached a peak value of $\sim 2 \times 10^{-4}$ S/m at a dose of ~ 0.1 dpa. Diagnostic measurements of the surface leakage resistances between the center, guard and back electrodes showed that this high apparent conductivity was not due to high surface leakage currents. The rapid increase in electrical conductivity of this specimen is very similar to the RIED behavior reported in several electron and ion irradiation studies [3,4,13-15]. However, continued irradiation to doses above 0.1 dpa resulted in a monotonic decrease in the electrical conductivity. The electrical conductivity decreased to $< 10^{-6}$ S/m by the middle of the third HFIR irradiation cycle (~ 2 dpa), which is only slightly larger than the initial RIC value for this specimen measured at the start of the first HFIR irradiation cycle. This "healing" of the high electrical degradation suggests that a physical process such as specimen microcracking [16] might have been responsible for the initial increase in conductivity. If microcracking were responsible for the initial conductivity increase, oxidation of the conducting layer in the crack could produce a subsequent decrease in conductivity. Postirradiation microstructural examination of this specimen is planned to provide further insight into possible physical mechanisms responsible for the initial increase and subsequent decrease in electrical conductivity.

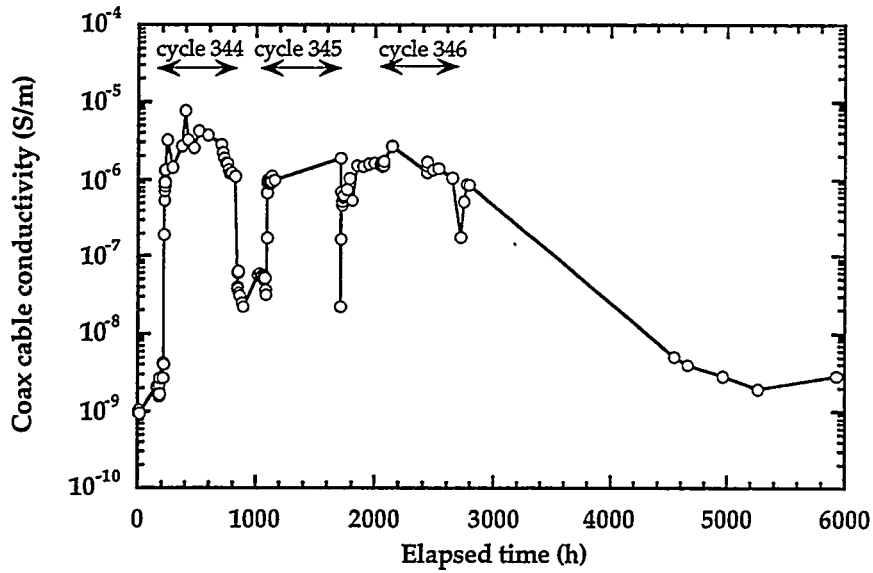


Fig. 5. Electrical conductivity of the MgO insulation in the coaxial cable for subcapsule #3 prior to, during and following the three HFIR irradiation cycles.

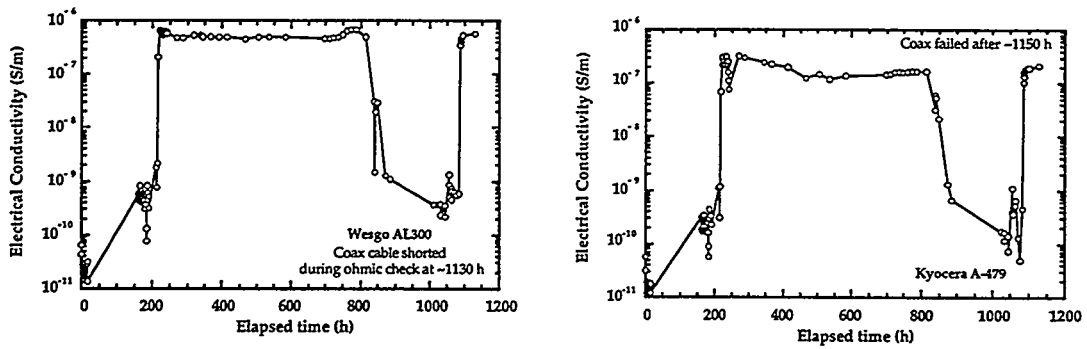


Fig. 6. Electrical conductivity of two polycrystalline alumina specimens (positions #7 and #8) before and during the first two HFIR irradiation cycles. Cycle 344 started at ~200 h and the reactor was shut down between 800 and 1100 h for normal core replacement operations.

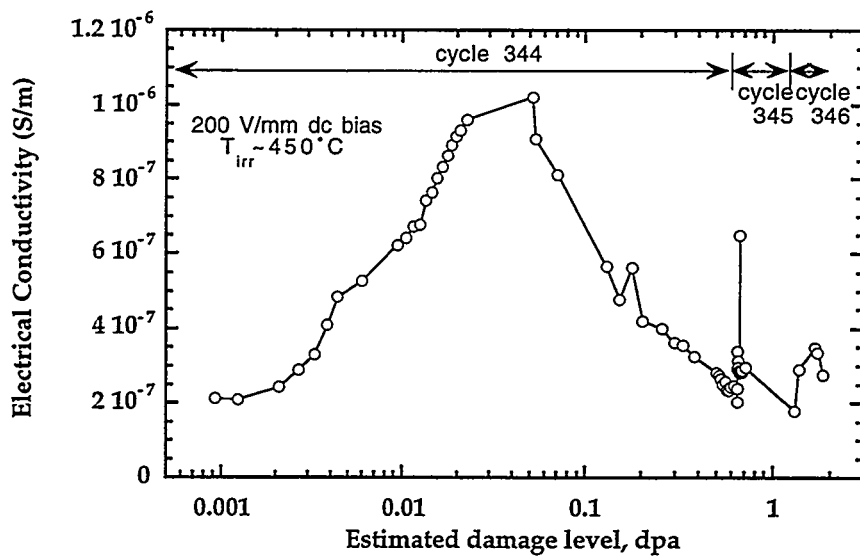


Fig. 7. Dose dependent electrical conductivity of UV grade Crystal Systems sapphire (position #2) during full-power HFIR irradiation.

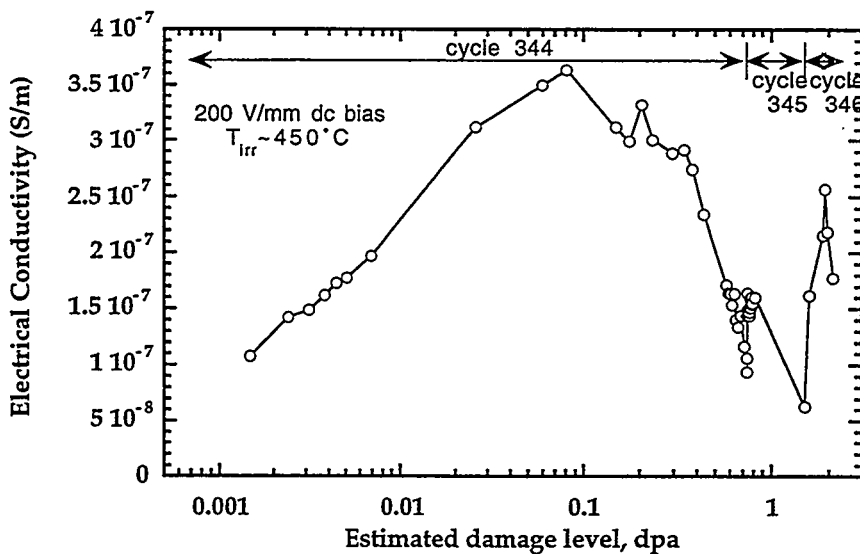


Fig. 8. Dose dependent electrical conductivity of regular grade Crystal Systems sapphire (position #3) during full-power HFIR irradiation.

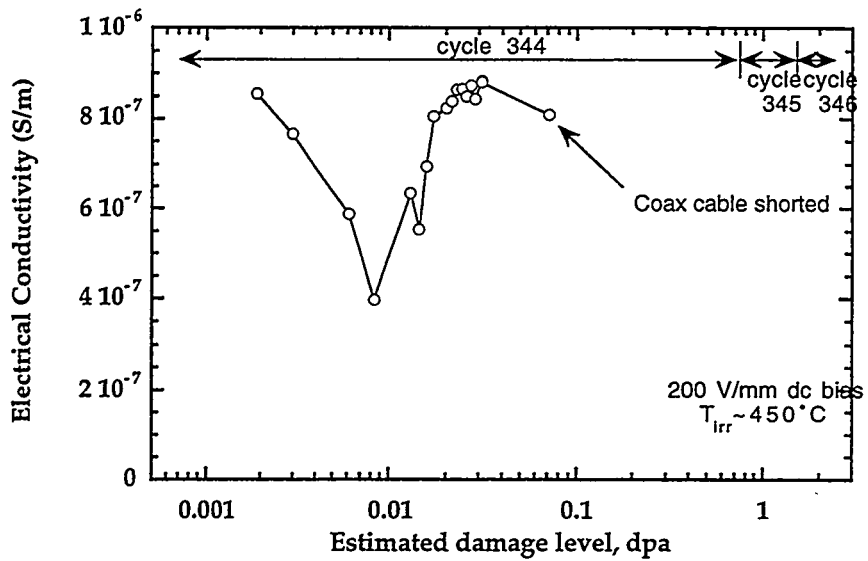


Fig. 9. Dose dependent electrical conductivity of Vitox alumina (position #5) during full-power HFIR irradiation.

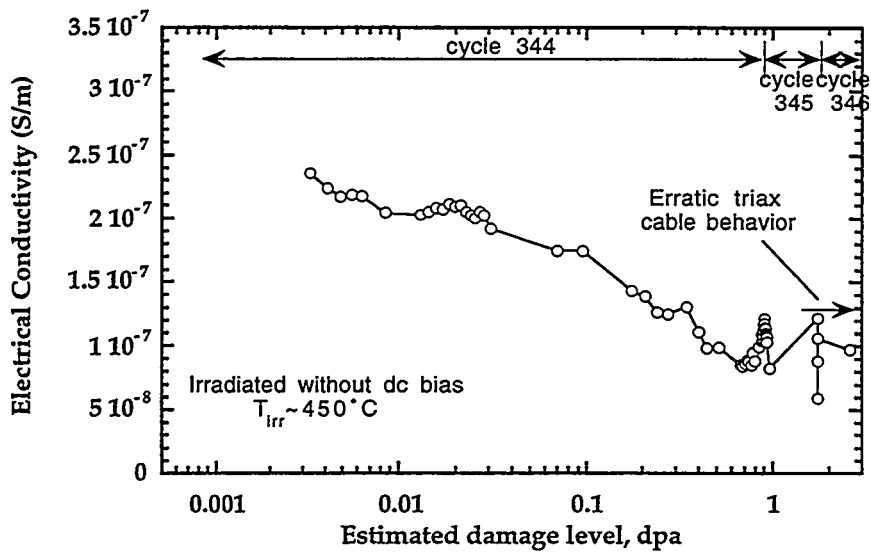


Fig. 10. Dose dependent electrical conductivity of Wesgo AL995 (position #11) during full-power HFIR irradiation. The specimen was irradiated without dc bias.

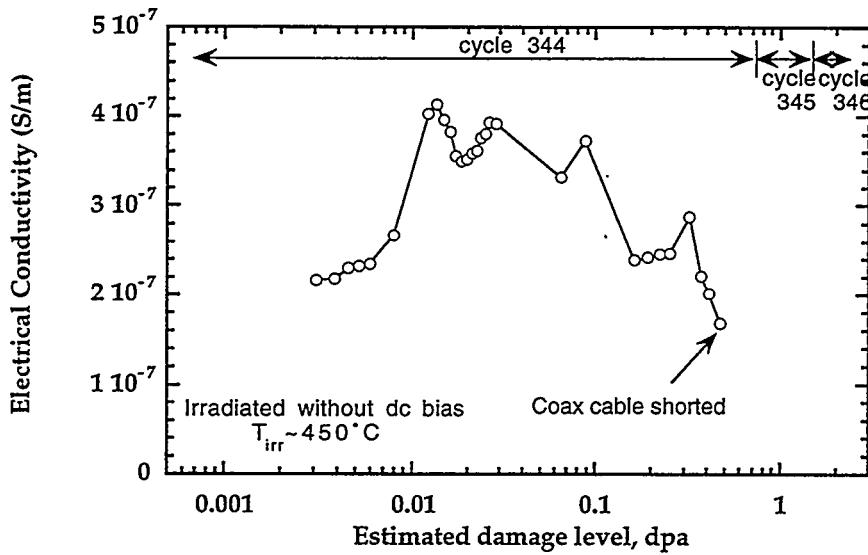


Fig. 11. Dose dependent electrical conductivity of regular grade Crystal Systems sapphire (position #12) during full-power HFIR irradiation. The coaxial cable failed near the end of the first HFIR irradiation cycle despite the fact that the specimen was irradiated without dc bias.

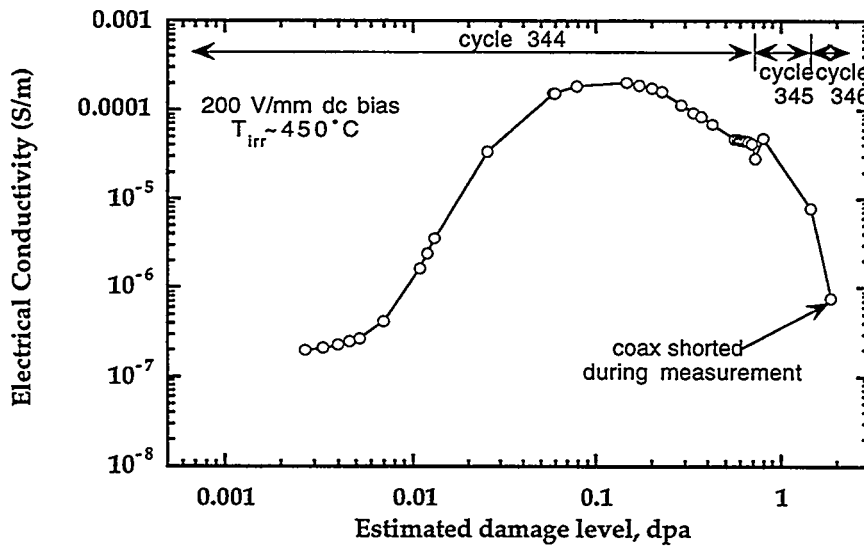


Fig. 12. Dose dependent electrical conductivity of 0.05% Cr-doped sapphire (position #13) during full-power HFIR irradiation.

Investigation of the dielectric breakdown strength of the HFIR TRIST-ER1 coaxial cables

A total of ten of the 15 coaxial cables in the HFIR TRIST-ER1 capsule failed by partial or full electrical short during the 3 1/2 month irradiation. It is worth noting that two of the electrical shorts in the coaxial cables occurred in unbiased specimens (cables for subcapsules 12 and 15, e.g., Fig. 10). This suggests that the cable failure was not associated with some type of RIED phenomenon. The biased coaxial cables were subjected to a dc potential of 150 V during the HFIR irradiation, which produced a maximum electric field of ~400 kV/m near the center conductor. All of the HFIR cables (biased and unbiased) were subjected to periodic electric measurements with potentials ranging from +100 V to -100 V (+150 V to -150 V in some cases).

The dielectric breakdown strength (DBS) of the MgO powder insulation used in the HFIR coaxial cables is expected to be comparable to the DBS for monolithic MgO, which has been measured to be ~100 MV/m at ~500°C and ~0.1 MV/m at 1200°C [17]. On the other hand, the dielectric breakdown strength of glass decreases from a typical value of ~100 MV/m at room temperature to <1 MV/m at temperatures above 200°C (depending on the particular grade of glass) [18]. The HFIR coaxial cables were sealed with Ferro 7556 lead borosilicate glass, which has a softening temperature of 330°C. The temperature-dependent dielectric breakdown strength of this grade of glass was not available from the glass manufacturer.

Experimental tests were performed on six unirradiated control coaxial MI cables from the HFIR TRIST-ER1 experiment in order to measure the dielectric breakdown strength of the cables. Since the dielectric breakdown strength of glass depends on both test temperature and the duration of the applied electric field, several different types of tests were performed. Most of the tests were performed at 200°C, which corresponds to the maximum expected operating temperature of the coaxial cables during full-power HFIR irradiation. For short term tests of the DBS, the voltage was applied for a time period of 0.5-1 min. If no shorting occurred, the voltage was increased by 50 V and the test was repeated. Table 4 summarizes the results of the dielectric breakdown tests. The DBS measured from short-term application of a constant-polarity voltage ranged from >1100 V (the maximum voltage for the Keithley 237 power supply) at room temperature to 850 V at 200°C. The DBS decreased to 500 V when the polarity of the applied potential alternated from positive to negative in short term tests. The DBS was approximately 300 V when the voltage was applied for several hours at a given potential. The dielectric breakdown was confirmed to occur in the glass seal region of the MI cables in all of these tests.

The measured dielectric breakdown strength of the glass seals in the control MI cables for the long term (>5 h) tests) is within a factor of two of the dc potential continuously applied to the 12 biased specimens in the HFIR TRIST-ER1 capsule. In addition, the measured DBS for the short term tests with alternating polarity is only about a factor of 5 larger than the voltages applied to all (biased and unbiased) of the HFIR specimens during ohmic check measurements. Therefore, it seems reasonable to assume that the shorting of the HFIR coaxial cables may be due to conventional dielectric breakdown in the glass seals (possibly assisted by some radiation-induced degradation in the glass). Postirradiation examination of the coaxial cables from the HFIR TRIST-ER1 experiment is planned in order to verify the cause of the shorting of the cables.

Table 4. Dielectric breakdown strength measurements on unirradiated HFIR coaxial MI cables.

T_{test}	Test condition	Dielectric breakdown strength
20°C	short term tests (≤ 1 min.), constant polarity	>1100 V (>2.8 MV/m)
200°C	"	850 V (2.2 MV/m)
200°C	short term tests, alternating polarity	~500 V (1.3 MV/m)
200°C	long term tests (>5 h), constant polarity	300 V (0.8 MV/m)
200°C	long term tests, alternating polarity	~300 V (0.8 MV/m)

Discussion and summary

Catastrophic radiation-induced electrical degradation ($\sigma_e > 10^{-4}$ S/m) was not observed in any of the HFIR-irradiated polycrystalline or high-purity sapphire specimens (~3 dpa maximum dose). As shown in Fig. 13, the measured RIC values for alumina are in good agreement with previous studies [2]. The quantitative level of RIC decreased slightly following irradiation in several of the specimens, in agreement with previous irradiation studies performed without an applied electric field during irradiation [19]. The decrease in conductivity has generally been attributed to increased electron-hole trapping at radiation-produced defects.

Previous studies of the RIED phenomenon have either used irradiation sources with very high ionizing radiation/dpa environments (electron and light ion irradiations) and/or were only performed to relatively low doses (e.g., less than ~0.5 dpa for JMTR fission reactor studies) [2]. The electron irradiation studies indicated that RIED would be most pronounced in high-purity single crystal specimens, and would be the least pronounced in low-purity polycrystal specimens [3]. In the TRIST-ER1 experiment, two single crystal specimens of alumina were successfully irradiated to the highest doses ever studied in an RIED experiment (>2 dpa). Previous RIED studies on single crystal alumina were limited to a maximum dose of 0.01 dpa [2]. The electrical conductivity of all specimens except for the Cr-doped sapphire (ruby) remained less than $\sim 1 \times 10^6$ S/m (i.e., at the normal RIC level) during extended full-power irradiation in HFIR. As discussed at a recent IEA workshop [20], there are several possible explanations for the discrepancy between the electron RIED studies and the present work. One possibility is that the large amount of implanted charge associated with electron irradiation may somehow trigger the initiation of RIED. Further work is needed to understand the physical mechanism(s) responsible for producing RIED in electron-irradiated samples.

A moderate amount of RIED that apparently is not due to surface leakage currents was observed in the Cr-doped sapphire specimen; the full-power conductivity increased by nearly 3 orders of magnitude after the first few days of irradiation and then gradually decreased over the ensuing 3 months. Further work is needed to determine the cause of the high apparent bulk conductivity of the ruby specimen which occurred at a dose of ~0.1 dpa.

Simple calculations suggest that the observed non-ohmic electrical behavior during HFIR irradiation is due to preferential attraction of ionized electrons in the capsule gas to the unshielded "low-side" electrical leads, but further analysis is needed to determine if this process can quantitatively explain the observed experimental data.

Shorting of many of the coax cables in the HFIR TRIST-ER1 capsule is attributed to dielectric breakdown of the glass used to seal the ends of the cables, based on tests performed on several non-irradiated control coax cables at 200°C. The dielectric breakdown strength (DBS) decreased with increasing temperature, and the breakdown was confirmed to occur in the glass terminations.

Disassembly of the HFIR TRIST-ER1 capsule is currently in progress. Several different post-irradiation measurements are planned, including electrical resistivity vs. temperature for all 15 alumina specimens and examination of the shorted coaxial cables. Microstructural examination of selected alumina specimens may also be performed.

REFERENCES

- [1] S.J. Zinkle et al., in Fusion Materials Semiannual Progress Report for Period ending June 30, 1996, DOE/ER-0313/20 (Oak Ridge National Lab, 1996) p. 257.
- [2] C. Kinoshita and S.J. Zinkle, J. Nucl. Mater. 233-237 (1996) 100.
- [3] E.R. Hodgson, J. Nucl. Mater. 212-215 (1994) 1123.
- [4] A. Möslang, E. Daum and R. Lindau, in Proc. 18th Symp. on Fusion Technology, eds. K. Herschbach, W. Naurer and J.E. Vetter (North-Holland, Amsterdam, 1994) p. 1313.

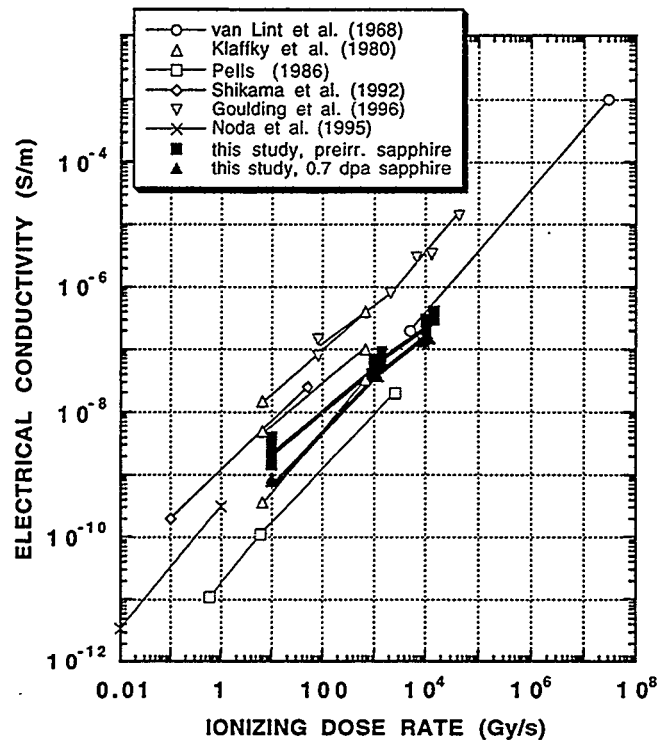


Fig. 13. Comparison of the electrical conductivity of high purity sapphire measured in the present study with previous studies on RIC in alumina.

- [5] S. J. Zinkle, in Fusion Materials Semiannual Progress Report for Period ending December 31, 1995, DOE/ER-0313/19 (Oak Ridge National Lab, 1995) p. 258.
- [6] A. L. Qualls et al., in Fusion Materials Semiannual Progress Report for Period ending June 30, 1996, DOE/ER-0313/20 (Oak Ridge National Lab, 1996) p. 267.
- [7] V.A.J. van Lint et al., Mechanisms of Radiation Effects in Electronic Materials, Vol. 1 (John Wiley & Sons, New York, 1980) p. 359.
- [8] F. J. Blatt, Physics of Electronic Conduction in Solids (McGraw-Hill, New York, 1968) p. 446.
- [9] J. G. Chervenak and V.A.J. van Lint, IEEE Trans. Nucl. Sci. NS-32 (1985) 4308.
- [10] J. G. Chervenak and V.A.J. van Lint, IEEE Trans. Nucl. Sci. NS-29 (1982) 1880.
- [11] F. F. Chen, in Plasma Diagnostic Techniques, eds. R. H. Huddlestone and S. L. Leonard (Academic Press, New York, 1965) p. 113.
- [12] W. Kesternich, F. Scheuermann and S. J. Zinkle, J. Nucl. Mater. 219 (1995) 190.
- [13] E. R. Hodgson, J. Nucl. Mater. 179-181 (1991) 383.
- [14] G. P. Pells, J. Nucl. Mater. 184 (1991) 177.
- [15] X.-F. Zong et al., Phys. Rev. B 49 (1994) 15514.
- [16] S. J. Zinkle, J. D. Hunn and R. E. Stoller, in Microstructure of Irradiated Materials, MRS Symp. Proc. vol. 373, eds. I.M. Robertson et al. (Materials Research Soc., Pittsburgh, 1995) p. 299.
- [17] K. L. Tsang, Y. Chen and J. J. O'Dwyer, Phys. Rev. B 26 (1982) 6909.
- [18] J. J. O'Dwyer, The Theory of Dielectric Breakdown of Solids (Oxford Univ. Press, 1964)
- [19] S. J. Zinkle and E. R. Hodgson, J. Nucl. Mater. 191-194 (1992) 58.
- [20] S. J. Zinkle, E. R. Hodgson and T. Shikama, in Fusion Materials Semiannual Progress Report for Period ending June 30, 1997, DOE/ER-0313/22, in press.